Spatial ordering in InP/InGaP nanostructures

J. R. R. Bortoleto, H. R. Gutiérrez, M. A. Cotta, J. Bettini, L. P. Cardoso, and M. M. G. de Carvalho

Articles you may be interested in

Highly polarized self-assembled chains of single layer InP/(In,Ga)P quantum dots
Appl. Phys. Lett. **97**, 253113 (2010); 10.1063/1.3529467

Shape dependent carrier dynamics in InAs/GaAs nanostructures
J. Appl. Phys. **106**, 113522 (2009); 10.1063/1.3267851

Self-assembled chains of single layer InP/(In,Ga)P quantum dots on GaAs (001)
J. Appl. Phys. **105**, 124308 (2009); 10.1063/1.3154023

Wavelength controlled multilayer-stacked linear InAs quantum dot arrays on InGaAsP/InP (100) by self-organized anisotropic strain engineering: A self-ordered quantum dot crystal
Appl. Phys. Lett. **93**, 131906 (2008); 10.1063/1.2993178

Strain and band edges in single and coupled cylindrical InAs/GaAs and InP/InGaP self-assembled quantum dots
J. Appl. Phys. **92**, 5819 (2002); 10.1063/1.1510167

Spatial ordering in InP/InGaP nanostructures

J. R. R. Bortoleto,[a] H. R. Gutiérrez, M. A. Cotta, J. Bettini, L. P. Cardoso, and M. M. G. de Carvalho

Instituto de Física Gleb Wataghin, DFA, UNICAMP, CP 6165, 13081-970 Campinas-SP, Brazil

We report the observation of a spatially-ordered bidimensional array of self-assembled InP quantum dots grown on slightly In-rich InGaP layers. The alignment of InP dots is observed along [100] and [010] directions. This effect is enhanced when 2° off vicinal substrates are used; it is also strongly dependent on growth temperature. Our results suggest that the density and size of CuPt-type atomically ordered regions as well as compositional modulation of InGaP layers play an important role on the spatial alignment of InP/InGaP quantum dots. © *2003 American Institute of Physics.* [DOI: 10.1063/1.1572553]

In multilayers of self-assembled quantum dots, both theoretical and experimental works[1–5] have shown that the vertical-strain-field transmission can lead to gradual improvement in size homogeneity and lateral ordering. This is the case of stacking in IV–VI materials, for which the elastic anisotropy may originate a highly ordered three-dimensional (3D) array of dots.[4,5] However, for SiGe/Si or III–V dot superlattices, the aligment is mainly along the growth direction, and the lateral ordering is much less pronounced.[2–5] In approaches for a single layer of dots,[6–11] some researchers have used a thin, tensile-strained interlayer[10] or the strain field of misfit dislocations[10,11] to promote lateral ordering of III–V semiconductor quantum dots. Both techniques can provide a surface with gridded trenches where the islands nucleate preferentially.

In this letter, we report the spontaneous formation of a bidimensional array of self-organized InP/InGaP dots for slightly In-rich InGaP layers. Our results show that the strain in the InGaP layer is a necessary, but not sufficient, condition to spatial dot alignment tendency. The formation of preferential sites for 3D island nucleation is related to the density and size of CuPt-type atomically ordered regions and/or compositional modulation, both observed in the InGaP buffer layer of our samples. Spatial ordering of InP dots depends on the size compatibility between dot radius and preferential surface regions for dot nucleation; this can be tuned by choosing the correct growth parameters.

The samples were grown by chemical-beam epitaxy on semi-insulating (001) GaAs substrates. Both nominally oriented and misoriented (2° off towards ⟨111⟩A, A-surface hereafter) substrates were used. Trimethylindium and triethylgallium, with H_2 as a carrier gas, were used as group-III sources. Thermally cracked AsH_3 and PH_3 were used as group-V sources. The substrate native oxide was removed by heating the sample at 600 °C under AsH_3 overpressure. For all samples presented here, a 300-nm GaAs buffer layer at 550 °C and growth rate of 0.72 μm/h, followed by a InGaP layer (thickness ranging from 10 nm to 450 nm) at a rate of 0.95 μm/h were grown. The growth temperatures for the InGaP layer were 540 and 550 °C. Subsequently, four mono-

layers (MLs) of InP were deposited at 540 °C and 0.2 ML/s. Surface morphology was investigated by atomic force microscopy (AFM), operating in noncontact mode with conical silicon tips. Fourier transform (FT) of the AFM images was used to characterize the lateral ordering of InP dots. The lattice mismatch ($\Delta a/a$) of InGaP layers was obtained from (004) rocking curves using double-crystal x-ray diffractometry (XRD). During the growth process the reflection high-energy electron diffraction (RHEED) pattern was monitored; the InGaP surface shows a (2×1) reconstruction for all samples. The 77-K photoluminescence (PL) peak energy of the InGaP layer, excited with the 514.5-nm line of an Ar+ laser, was used to determine the degree of CuPt ordering in these samples. Cross-section transmission electron microscopy (XTEM) and transmission electron diffraction (TED) images were obtained using a JEM 3010 URP 300-kV TEM. TED images were used as complementary tool to observe CuPt ordering in InGaP layers.

Table I presents the growth conditions and InGaP layer properties for each sample. For this set of samples, partially ordered InGaP layers are grown. InGaP layers grown on (001) GaAs usually show the $CuPt_B$ ordering, which consists of alternating In-rich and Ga-rich planes along [$\bar{1}$11] and [1$\bar{1}$1] directions.[12–15] The degree of $CuPt_B$ ordering in lattice-matched InGaP films was characterized using the equation[14] $\eta = \sqrt{(PL^0 - PL_{peak})/0.471}$, where the PL peak of completely disordered InGaP alloys was assumed to be $PL^0 = 1.992$ eV. This value agrees with previous work of

TABLE I. Growth temperature (T), V/III ratio, strained mismatch ($\Delta a/a$), rms roughness calculated from 2-μm×2-μm AFM scans and PL peak energy for InGaP layers grown on nominal substrates. V/III ratio variation was obtained by changing the PH_3 flux only; all InGaP layers shown here are 450 nm thick. Run-to-run fluctuations in the InGaP composition provided mismatch variations smaller than ±0.05%.

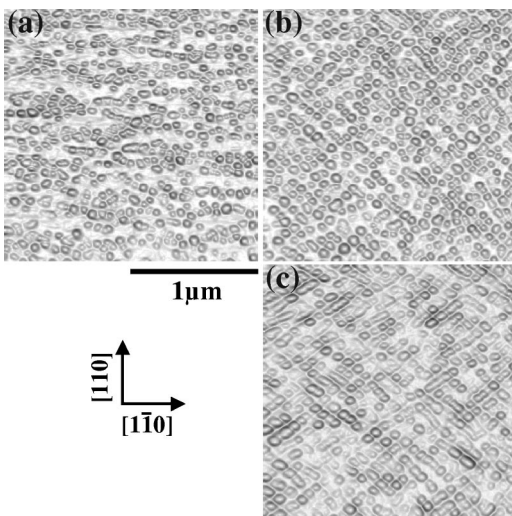| Sample	T (°C)	V/III ratio	$\Delta a/a$(%)	Rms (nm)	PL peak (eV)
1	540	17	<0.01	0.905	1.948
2	540	17	0.40	0.295	1.931
3	550	17	<0.05	0.363	1.967
4	550	17	0.60	0.165	1.929
5	550	32	<0.01	0.585	1.958
6	550	32	0.66	0.334	1.913

[a]Electronic mail: jrborto@ifi.unicamp.br

FIG. 1. AFM images showing the spatial distribution of InP/InGaP dots for (a) sample 1 grown on nominal substrate, sample 4 grown on (b) nominal and (c) A-surface GaAs substrates. The dots in sample 1 were grown on a lattice-matched InGaP layer, while for sample 4 the InGaP was 0.60% mismatched to the GaAs. The gray scale in the images means the projection of the local surface normal onto the growth plane. Darker regions correspond to steeper facets.

DeLong *et al.*[15] The less atomically ordered sample studied in our case, which still shows extra $\{1/2,1/2,1/2\}$ spots in TED pattern, presents a PL peak ~ 1.967 eV. In this way, the ordered phase volume corresponds to 20–30% of the grown material for the growth conditions used here. On the other hand, dark-field measurements ($g = 2\bar{2}0$) of the InGaP buffer layers show periodic dark/bright contrast that have usually been attributed in literature to compositional modulation.[16–19]

Figure 1(a) shows a typical AFM image of InP dots grown on a GaAs lattice-matched InGaP layer (sample 1). No clear alignment of the dots can be observed. However, a bidimensional self-organized array of dots is clearly observed in Fig. 1(b) (sample 4). The array of dots is roughly aligned at [010] and [100] directions. This spatial arrangement occurs homogeneously on the whole sample surface and is more clearly observed for samples grown under the same conditions on A-surfaces [shown in Fig. 1(c)]. The In-GaP layer for sample 4 is slightly In-rich, approximately 0.6% mismatched, and was grown at 550 °C. No spatial organization was observed for InP dots grown on lattice-matched InGaP layers at 550 °C, either on nominal or vicinal substrates. The dot density is around 1.6×10^{10} cm^{-2} for all our samples.

Since InP layer growth conditions were the same for the whole sample set, the kinetic effects could be dismissed as the main cause for the bidimensional array of dots observed in sample 4. In Fig. 2, we present the FTs for $3-\mu$m $\times 3-\mu$m AFM images of the samples listed in Table I. We can see that both V/III ratio and growth temperature for the InGaP buffer layer strongly influence the lateral ordering tendency of InP dots. Figure 2 also shows that the strain in InGaP layer is a necessary condition to a clear spatial dot alignment tendency. Thus the dot nucleation must be related to strain field relaxation in the InGaP layer, either coherent[9] or incoherently.[10] In our case, the InGaP layer thickness and mismatch are below the critical value for misfit dislocation
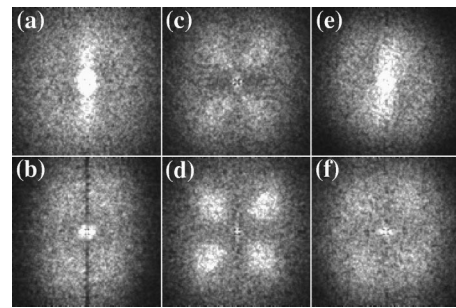

FIG. 2. FT power spectrum of $3-\mu$m$\times 3-\mu$m AFM scans for samples listed in Table I: (a) to (f) refer to samples 1 to 6, respectively.

formation;[20] therefore, still within ideally strained epilayer range. Moreover, $\langle 110 \rangle$ and [010] cross-sectional dark-field measurements (not shown) indicate that our samples are dislocation free. Therefore, a likely explanation for the spatial InP dot arrangement is a lateral modulation of the strain field associated to the slightly mismatched InGaP layer. From Fig. 2 we can see that this strain-field modulation can be obtained for a narrow range of growth conditions.

AFM images in Fig. 3 show morphologies of InGaP layers grown simultaneously on nominal [Fig. 3(a)] and A-surface [Fig. 3(b)] GaAs substrates. In this case, the growth parameters were similar to those for sample 4, where the dots are spatially well organized. The InGaP layer grown on the nominal substrate shows a smooth surface typical for InGaP growth, where faint alignment of the terraces but no trenches can be observed. The height profile of the dashed line indicates that only steps up to 0.6 nm form on the surface. Figure 3(b), however, shows a more striking surface structure. A bidimensional surface corrugation (up to 1 nm high) is present on the top of the InGaP layer. The period of the corrugation (~ 60–70 nm) is essentially the same as the island size for the sample with InP dots. It is important to point out that InP dot spatial alignment was observed for both InGaP surfaces shown in Fig. 3, although this effect was stronger for the A-surface substrate. Thus the presence of a
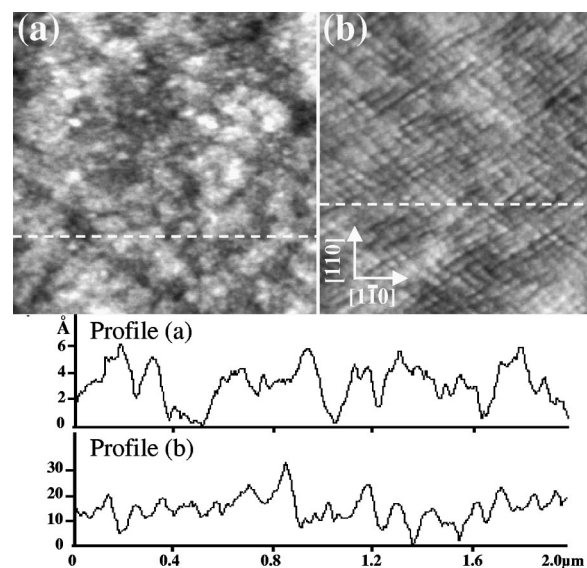

FIG. 3. AFM images of 450-nm-thick InGaP surfaces grown simultaneously on (a) nominal and (b) A-surface GaAs substrates at conditions that promote alignment of InP dots (sample 4).

stepped surface can enhance InP dot spatial organization, suggesting that surface effects are important to determine the strain-field modulation.

The origin of the InP dot arrangement in our samples may be related to the interaction of the strain field in the InGaP layer with two other phenomena, $CuPt_B$ ordering and/or compositional modulation both strongly dependent on surface configuration. Several works point out that the growth conditions influence the $CuPt_B$ order by changing the concentration of $[1\bar{1}0]$ P dimers on the reconstructed surface.[12,13] Also, it has been proposed that $CuPt_B$ InGaP layers present an In-rich surface.[12] The surface corrugation shown in Fig. 3(b) could thus be due to In-rich plateaus formed by surface segregation that occurs with surface reconstruction. These results suggest that the corrugated pattern on A-surface and spontaneous formation of InP dot arrays can originate from an interplay between the strain field in the layer and the arrangement of ordered regions within the InGaP volume. Indeed, a minimum InGaP thickness (larger than 30 nm) is necessary to align the InP dots grown at 550 °C. This can be understood either as a minimum strain field and/or a minimum ordered region size necessary to create the bidimensional surface modulation. Moreover, the size compatibility of atomically-ordered regions and InP dots should likely vary with the degree of $CuPt_B$ order in the InGaP layer, which determines the size of In-rich plateaus.

Compositional modulation could also trigger a periodic strain field and consequently preferential sites for dot nucleation. However, the correlation between compositional modulation and surface morphology is not well established experimentally in literature.[16–18] It has been proposed that it strongly depends on the growth conditions,[19] which determine stable (smooth surfaces) and unstable (corrugated surfaces) growth modes. In our case, XTEM dark-field measurements with $g=2\bar{2}0$ show dark and bright regions. For samples with a low-degree of InP dot spatial organization (i.e., sample 1) the dark/bright regions are randomly distributed and no periodic contrast can be clearly established. On the other hand, for samples with a clear spatial arrangement of dots (sample 4), the dark/bright regions are larger and periodically distributed along the $\langle 110 \rangle$ directions, with a wavelength in the range of 40–70 nm, closer to the mean distance in between dots (70 nm). A detailed study of TEM measurements will be published elsewhere. However, clear bidimensional dot arrangements were obtained when InP was grown on smooth InGaP buffer layers (rms roughness <0.2 nm). Thus, if compositional modulation occurred, the growth mode should provide stable, smooth surfaces, like those observed for all InGaP thicknesses used here.

In summary, we observe the formation of a spontaneous bidimensional array of self-organized InP dots when grown on slightly In-rich InGaP layers. Our results show that the strain in the InGaP layer is not the only condition to spatial dot alignment tendency, since it strongly depends on growth temperature and V/III ratio. This alignment is enhanced on A-surface substrates. Size compatibility between the InP dots and preferential regions for dot nucleation created by atomic ordering and/or compositional modulation of InGaP layers could explain this bidimensional InP dot arrangement. From the technological point of view, the tuning of ternary buffer layer growth conditions is an alternative path to obtain highly organized two-dimensional quantum-dot arrays.

[1] Q. Xie, A. Madhukar, P. Chen, and N. P. Kobayashi, Phys. Rev. Lett. **75**, 2542 (1995).

[2] J. Tersoff, C. Teichert, and M. G. Lagally, Phys. Rev. Lett. **76**, 1675 (1996).

[3] C.-S. Lee, B. Kahng, and A.-L. Barabási, Appl. Phys. Lett. **78**, 984 (2001).

[4] G. Springholz, V. Holy, M. Pinczolits, and G. Bauer, Science **282**, 734 (1998).

[5] V. Holý, G. Springholz, M. Pinczolits, and G. Bauer, Phys. Rev. Lett. **83**, 356 (1999).

[6] C. A. C. Mendonça, M. A. Cotta, E. A. Meneses, and M. M. G. Carvalho, Phys. Rev. B **57**, 12501 (1996).

[7] C.-S. Lee and A.-L. Barabási, Appl. Phys. Lett. **73**, 2651 (1998).

[8] F. Hatami, U. Müller, H. Kissel, K. Braune, R.-P. Blum, S. Rogaschewski, H. Niehus, H. Kirmse, W. Neumann, M. Schmidbauer, R. Köhler, and W. T. Masselink, J. Cryst. Growth **216**, 26 (2000).

[9] Z. Jin, B. Wang, Y. Peng, F. Zhao, W. Chen, S. Liu, and C. Gao, Surf. Sci. **423**, L211 (1999).

[10] K. Häusler, K. Eberl, F. Noll, and A. Trampert, Phys. Rev. B **54**, 4913 (1996).

[11] A. E. Romanov, P. M. Petroff, and J. S. Speck, Appl. Phys. Lett. **74**, 2280 (1999).

[12] A. Zunger, MRS Bull. **22**, 20 (1997).

[13] M. Zorn, P. Kurpas, A. I. Shkrebtii, B. Junno, A. Bhattacharya, K. Knorr, M. Weyers, L. Samuelson, J. T. Zettler, and W. Richter, Phys. Rev. B **60**, 8185 (1999).

[14] P. Ernst, C. Geng, F. Scholz, H. Schweizer, Y. Zhang, and A. Mascarenhas, Appl. Phys. Lett. **67**, 2347 (1995).

[15] M. C. DeLong, D. J. Mowbray, R. A. Hogg, M. S. Skolnick, J. E. Williams, K. Meehan, S. R. Kurtz, J. M. Olson, R. P. Schneider, M. C. Wu, and M. Hopkinson, Appl. Phys. Lett. **66**, 3185 (1995).

[16] O. Ueda, S. Isozumi, and S. Komiya, Jpn. J. Appl. Phys. **23**, L241 (1984).

[17] T. Okada, G. C. Weatherly, and D. W. McComb, J. Appl. Phys. **81**, 2185 (1997).

[18] F. Peiró, A. Cornet, J. R. Morante, A. Georgakilas, C. Wood, and A. Christou, Appl. Phys. Lett. **66**, 2391 (1995).

[19] B. J. Spencer, P. W. Voorhees, and J. Tersoff, Appl. Phys. Lett. **76**, 3022 (2000).

[20] K. Ozasa, M. Yuri, S. Tanaka, and H. Matsunami, J. Appl. Phys. **68**, 107 (1990).